Effects of Instream Boulders on Bedload Transport

Eric DeWitt, Research Assistant, Clarkson University, Potsdam, NY, dewittek@clarkson.edu
Abul B. Baki, Assistant Professor, Clarkson University, Potsdam, NY, abaki@clarkson.edu
Weiming Wu, Professor, Clarkson University, Potsdam, NY, wwu@clarkson.edu

Abstract

Boulder arrangements, as a measure of stream restoration, have been known to significantly impact the local sediment transport around the elements as well as the reach-averaged sediment transport in the channel. The present experimental study explores how the boulder spatial density and bed slope affect bedload transport in a channel. Boulders with 4 spatial densities of 0 (no boulder), 3.4%, 5.4%, and 8.3% were partially submerged into a mobile gravel bed in a flume. Each boulder density was repeated at 3 different bed slopes: 0.5%, 1.0%, and 1.5%. Flow discharge varied from 55 to 80 L/s. Bedload transport was recorded with a sediment trap at the flume exit and the water depth was recorded to calculate the bed shear stress. A formula is developed to predict the bedload transport rate in the channel with boulders.

Introduction

Sediment transport is a crucial driver in determining river morphology as well as the potential for riverine flooding, bank erosion, and habitat suitability for species living within the riverine ecosystems that blanket large parts of the world (Lamb et al. 2008). Many natural channels experience significant bedform changes due to large hydrological events. The presence of large immobile boulders or similar obstructions has been noted as a significant factor in bedload transportation and geomorphological changes (Ghilardi and Schleiss 2011). Rock ramps are a type of fish pass that consists of steep reaches stabilized by large roughness elements (LREs) to create suitable habitats for a desired fish species. Rock ramp designs have become a prevalent river restoration practice that reduces flow velocities, increases water depth, and dissipates energy (Baki et al. 2014). Instream LREs have a significant impact on local flow conditions in the vicinity of the LRE. There have been contradictory theories regarding the presence of LREs on sediment transport rates. Some propose that LREs will decrease the bedload transport rate by causing local accelerations and decelerations in the flow resulting in hydraulic jumps, large vertical velocities, increased local turbulence, and eddies within the water profile with weak net flow resulting in overall less available shear stress and energy available for sediment transport (Yager et al. 2007) (Ghilardi 2014b). However, some claim sediment transport may increase with the presence of boulders due to the additive nature of flow structures between small spacings of boulders, which increases erosion (Tan et al. 2012). Additionally, the effect of spacing between boulders on the bedload transport has also been experimentally investigated. Multiple papers have noted contradictory findings regarding the effects of boulder spacing on bedload transport. Some conclude that an increase in spacing results in a decrease in sediment transport (Ghilardi et al. 2014a, Papanicolaou et al. 2018), while other studies concluded that an intermediate spacing was ideal for a decrease in sediment transport (Hassan and Reid 1990, Yager et al. 2007). This study is focused on exploring the relationship between boulder placement and bedload transport of the channel that may provide better insight into rock ramp design to limit local erosion or increased sediment transport within the channel.

Experimental Methods

The Ecohydraulics flume at Clarkson University was used in this study to evaluate the sediment transport rate in the presence of boulders. It is a recirculating flume with a length of 13 m, a width of 0.96 m, a depth of 0.6 m, and a fixed gravel bed slope of 0.005 (Figure 1). The water is pumped into a basin and then enters the flume where two rectangular weirs are installed to provide controlled flow into the flume channel. The fixed gravel bed is 50 mm thick with a median gravel size (D_{50}) of 6.1 mm. An additional layer of mobile gravel with a D_{50} of 7.29 mm was set on top of the bed to adjust the bed slope. Grain size distribution of the mobile sediment was performed with 4 sieves with nominal sieve openings of 14, 12.5, 9.5, and 4.75 mm. The first and last meter of mobile gravel was fixed with glue at the entrance and the exit of the flume. This was intended to prevent erosion due to the freefall flow at the exit as well as flow over the weir at the entrance to the channel. No notable hydraulic structures were observed forming at either of these fixed bed points. A sediment trap is located at the outlet of the flume with two removable compartments resting on top of each other to allow for continuous measurements while one was removed to record the collected mass.

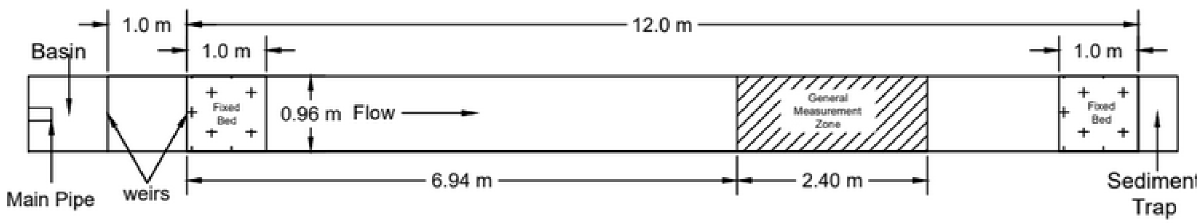

Figure 1. A simplified planimetric view of the flume

The experiment was conducted to assess the effect of LRE areal density on bedload transport. Four boulder scenarios were tested with the following boulder areal densities: $\lambda = 0$ (no boulder), 3.4, 5.4, and 8.3%. The planimetric view of the boulders for each scenario is shown in Figure 2. Semi-spherical natural boulders were used, with approximate diameters in the x (length) and z (height) directions of 12 and 10 cm, respectively. Boulders were submerged into the sediment layer 3 cm or having a protrusion of roughly 70% of the diameter.

The mobile layer on the bed surface was reset for each experiment to avoid compaction and transport-induced sediment rearrangement and sorting. The sediment depth varied from the entrance to the end of the flume to achieve the desired slope. Three bed slopes of 0.5%, 1%, and 1.5% were tested. The bed was wetted prior to a main flow with a hose to prevent potential impulse effects on the loose gravel. The two removable sediment traps were rotated to continuously collect sediment leaving the flume: one recording the steady flow and one recording the transition period. The sediment was emptied into a container on a balance and the mass was recorded. Water heights were taken at each flow rate with a pointer gauge at an equidistant point between boulders to limit the effect of local erosion and deposition near boulders. Preliminary trials were performed to identify a flow range that would effectively show a full range of increasing sediment transport rates. Additionally, these preliminary trials determined that a smaller recording duration would be required to allow the sediment traps to be removed without too much physical difficulty and to record the sediment within the trap. The flow in the flume began at 55 L/s and was run for 5 minutes to fully develop before any data was taken. The flow would run for 2.5 minutes and then was increased by 2.34 L/s (this value corresponds to an increase of 1 hz for the frequency of the pump used in the flume). This duration was similar to the process performed by McKie et al. (2021). A 30-second transition period was used between the intervals to allow ample time for the removal of the sediment traps and for measuring the mass within the traps. The flow rate was increased to 80 L/s, resulting in 11 separate flow rates. At the slope of 1.5%, the flow was only increased to a flow rate of 75 L/s due to the large transport and erosion occurring in the flume.

Table 1. Description of boulder scenarios

Experiment	Number of boulders	Boulder areal density (λ)	Total area GMZ* (m^2)	Area of boulders (m^2)	Area of mobiles (m^2)
S1	0	0	2.304	0	2.304
S2	7	0.0344	2.304	0.0792	2.2248
S3	11	0.0540	2.304	0.1244	2.1796
S4	17	0.0834	2.304	0.1923	2.1117

*-GMZ denoted general measurement zone

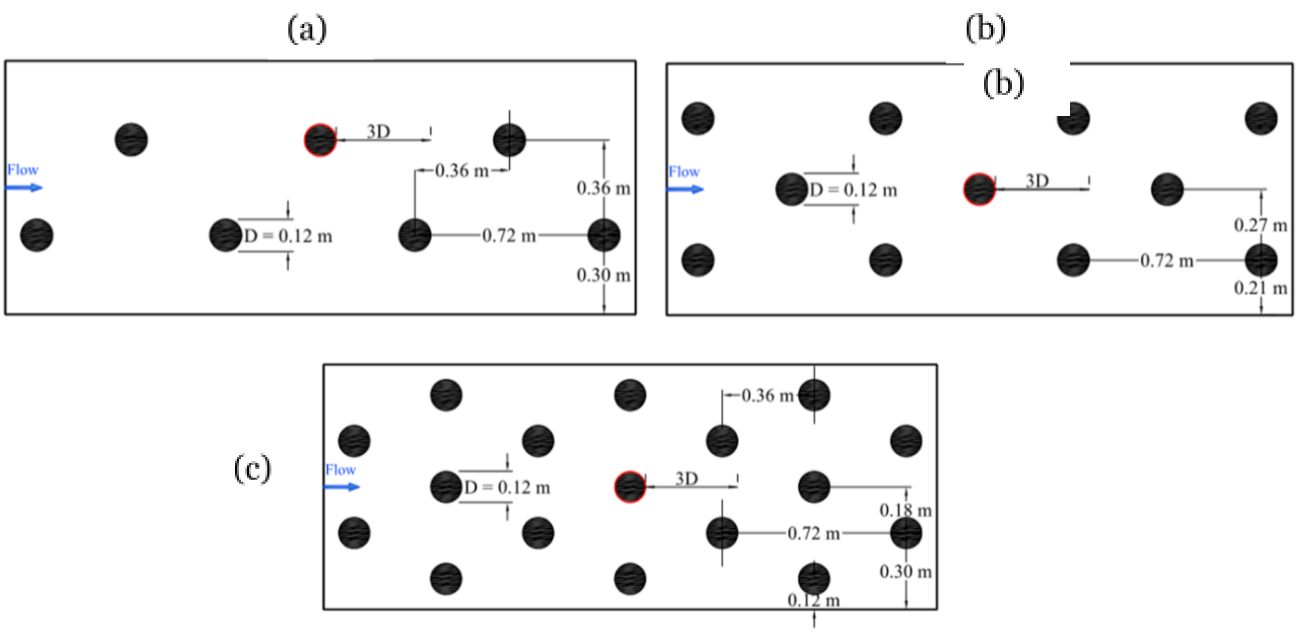

Figure 2. Boulder arrangements in the GMZ (a) Scenario S2 (λ = 3.4%), (b) Scenario S3 (λ = 5.4%), and (c) Scenario S4 (λ = 8.3%)

Results

The unit bedload transport rate, q_b, was obtained by dividing the recorded sediment mass by the exact duration and flume width for each flow discharge. Figure 3 shows the measured bedload transport rates for 0.5% (a), 1% (b), and 1.5% (c) channel slopes with varying flow discharges and varying boulder densities. Of the three boulder scenarios at each slope, S2 (λ = 3.44%) has the lowest bedload transport rate, while increasing the boulder areal density in S3 (λ = 5.4%) and S4 (λ = 8.34%) generally resulted in higher transport rates. The bedload transport was the lowest in the case of S1 (no boulder scenario) at the first tested flow rates (55-60 L/s), but exhibited different trends in the scenarios with LREs at higher flow discharges. The presence of boulders increased the transport rate from S1 in the low slope tests but decreased in the high slope tests at high flow discharges. The increase in flow affected the bedload transport more significantly in S1 than with the presence of LREs. Local velocity data were not recorded, so it is unable to confidently claim that this is due to the boulders dissipating energy and reducing the flow velocity of the channel. However, previous studies have demonstrated the validity of these claims (Baki et al. 2014; Ghilardi et al. 2014a). The variation of bedload transport due to the presence of LREs is dependent on the change in bed shear stress when LREs are introduced into the channel (Golpira 2022).

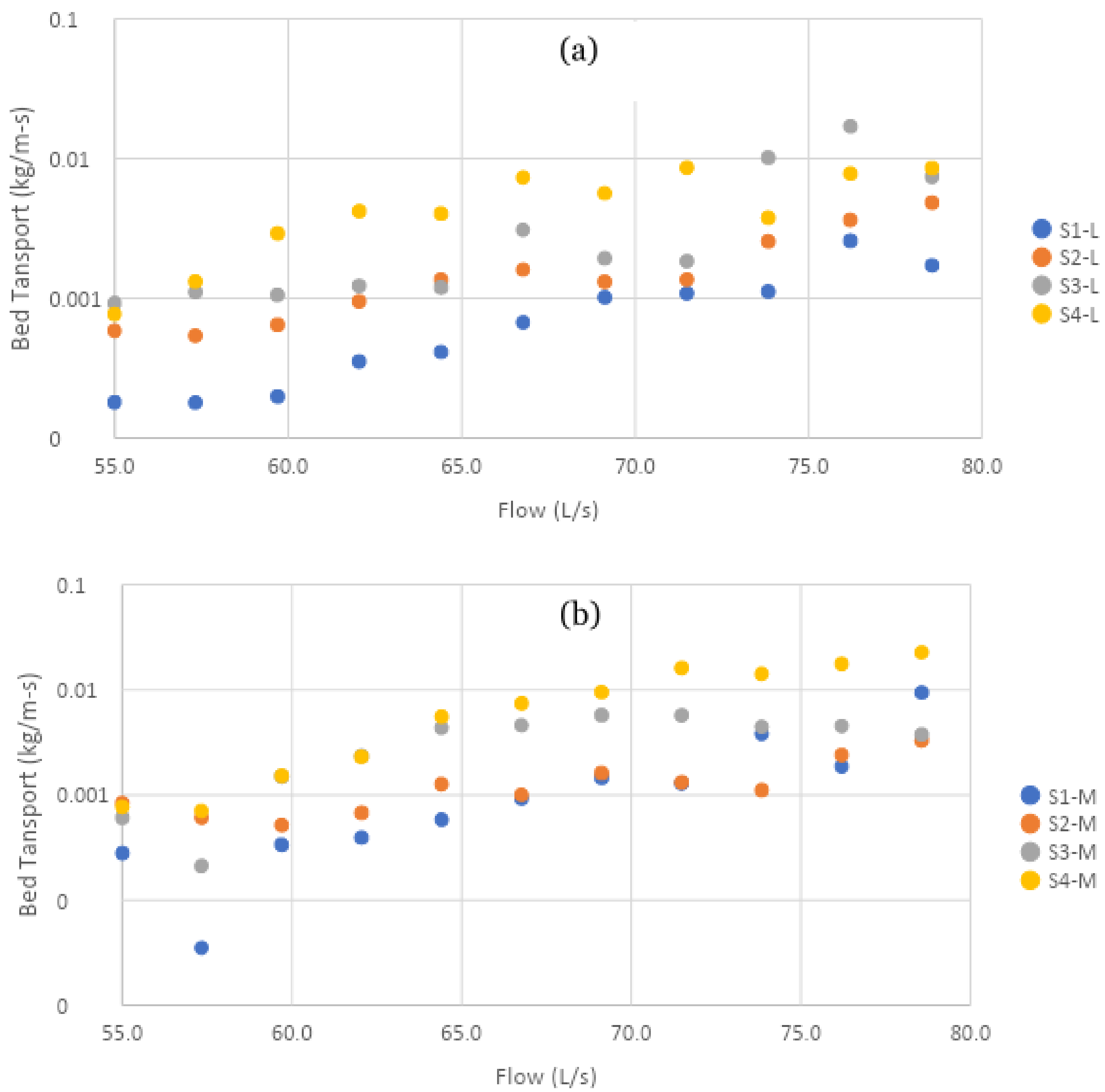

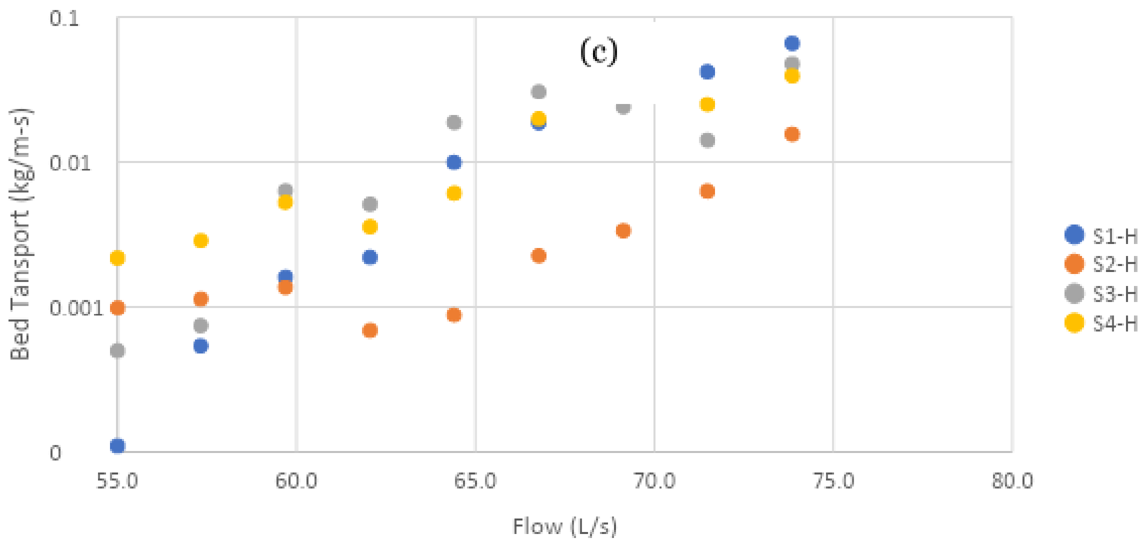

Figure 3. Measured bedload transport rates for varying flow discharges over (a) 0.5%, (b) 1.0%, and (c) 1.5% slopes

The bed shear stress values in each scenario are evaluated to identify a relationship between the transport rate and bed shear stress. Both variables are nondimensionalized. The dimensionless bedload transport rate, i.e., the Einstein number, is defined as

$$\Phi = q_b/[\rho_s\sqrt{\left(\frac{\rho_s}{\rho} - 1\right)gD^3}] \quad (1)$$

where q_b is bed transport per unit width (kg/m-s); ρ_s and ρ are the densities of sediment and water, respectively; D is the grain size of the sediments, set as D_{50}; and g is the acceleration of gravity, 9.81 m²/s. The sediment density ρ□ is estimated as 2650 kg/m³. The density of water at 20℃ is 998 kg/m³.

The Shields parameter is used as a dimensionless bed shear stress:

$$\Theta = \tau_m/[(\gamma_s - \gamma)D] \quad (2)$$

where τ_m is bed shear stress of the mobile particles (N/m²), γ_s is the specific weight of sediment, and γ is the specific weight of water.

The bed shear stress is calculated with the method proposed by Yager et al. (2007), which partitions the total reach-averaged shear stress, τ_t, into two portions: shear stress on the immobile boulders, τ_I, and shear stress on the mobile sediment particles, τ_m:

$$\tau_t A_t = \tau_I A_{IP} + \tau_m A_m \quad (3)$$

Where A_t, A_{IP}, and A_m are the bed areas corresponding to the three shear stresses. A_t is calculated as the length of the GMZ (L) multiplied by the channel width (b). A_{IP} is the planform area of boulders and evaluated as $A_{IP} = N \times \frac{\pi}{4} D^2$. A_m denotes the area of mobile sediment, calculated as the difference between the total area and the planform area of boulders: $A_m = A_t - A_{IP}$. The total reach-averaged shear stress is calculated as $\tau_t = \rho g h_a S$, which uses the slope and the calculated reach-averaged flow depth with $h_a = V_w / A_t$. V_w is the volume of water in the channel, found by subtracting the total volume of the boulders (V_i) from the total volume in the general measurement zone. V_i is determined by the equation $V_i = N \times \frac{\pi}{6} \times \left(D^3 - 3 \times Z_m^2 D + 2Z_m^3\right)$, where Z_m is the length of the submerged boulder and D and N denote the boulder diameter and number of boulders, respectively. The boulder shear stress is calculated as

$$\tau_I = \frac{\rho A_{IF} C_I U^2}{2A_{IP}} \quad (4)$$

where U is the reach-averaged flow velocity calculated with $U = \frac{Q}{V_w \times b / A_t}$, A_{IF} is the frontal area of boulders, and C_I is the drag coefficient of the boulders given the constant value of 0.5. This value is an average experimental value reported by Golpira (2022). The frontal areas of the boulders are given by $A_{IF} = N \times D \times (D - Z_m)$.

Equation (3) is rearranged as follows to calculate the bed grain shear stress:

$$\tau_m = \frac{\tau_t A_t - \tau_I A_{IP}}{A_m} \quad (5)$$

To converge the data across the various slopes, the Shields number is replaced with $\frac{\theta}{\theta_{ref}}$, where θ_{ref} is the reference Shields number. Schneider et al. (2015) determined that the reference Shields number has the following relationship for channel slopes steeper than 1%:

$$\theta_{ref} = 0.56 \times S^{0.5} \quad (6)$$

Figure 4 shows the relationship between the Einstein number and with $\frac{\theta}{\theta_{ref}}$, with θ_{ref} given by Equation (6) for the 1% and 1.5% slopes. A reference shear stress of 0.03 was used for the 0.5% slope dataset; 0.03 is an experimental value established as a low threshold from Wu et al. (2000). The relationship is represented by the following power regression function with a R^2 (coefficient of determination) value of 0.5337:

$$\phi = 0.000256 \times \left(\frac{\theta}{\theta_{ref}}\right)^{2.475} \quad (7)$$

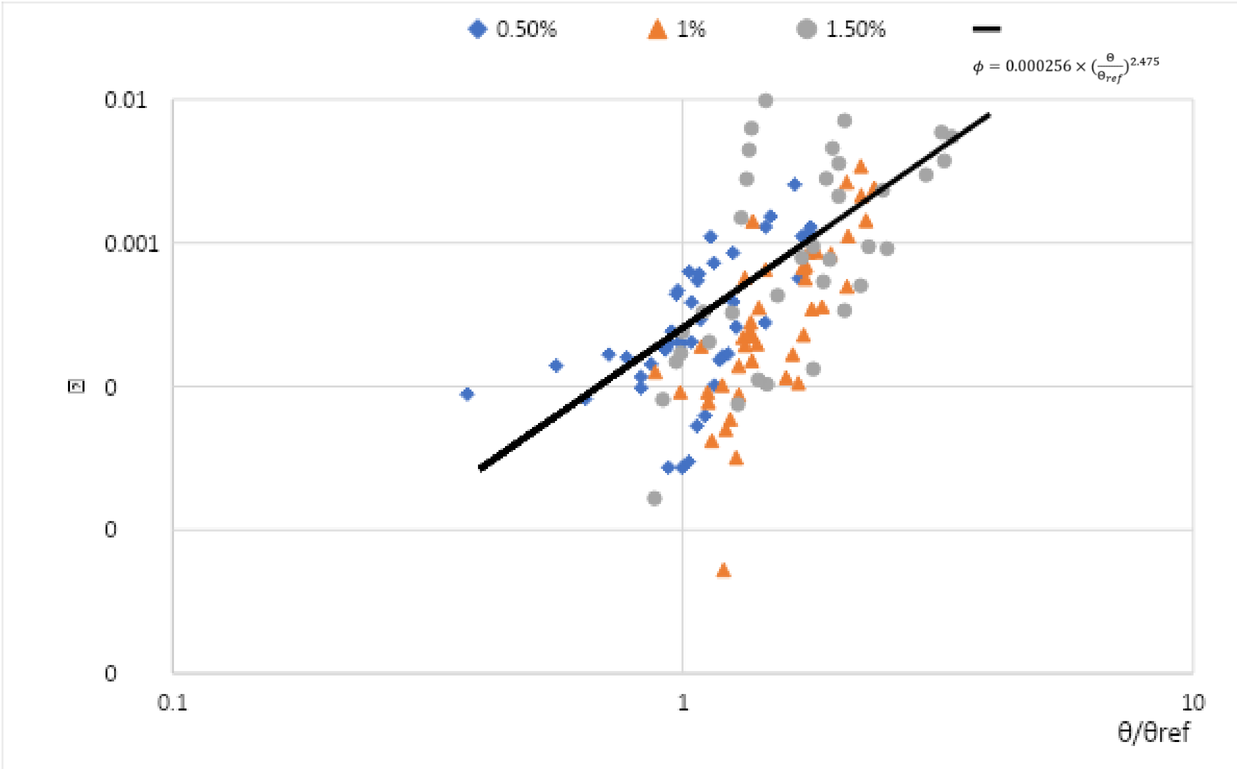

Figure 4. Shields number and Einstein number for each scenario by slope with the generated relationship between the bedload transport rate and $\frac{\theta}{\theta_{ref}}$

Figure 5 compares the measured (from experiments) and predicted (from Eq. 7) dimensionless bedload transport rates. The values of Einstein's number using the existing formulas of Paintal (1971) and Wu et al. (2000) are included for reference. Both formulae have been accepted for open channels without obstructions, and the large variations from the predicted-measured plot depict high discrepancies from what was observed in this experiment. All three datasets use slightly varying independent variables, but all evaluate the Einstein number. The formula of Wu et al. (2000) uses a critical Shields number ratio. If the recorded Shields number is below the critical value of 0.03, the bedload transport rate is equivalent to zero. This formula provides reasonable values for Shields numbers higher than the critical Shields number but has errors in the proximity of incipient motion. The formula of Paintal (1971) has large errors due to using the total bed shear stress as opposed to grain shear stress or shear stress of the mobiles. The generated equation agrees with the measurements from this limited data stronger than the two existing formulae, which is in part to being generated for the use of channels with the presence of LREs.

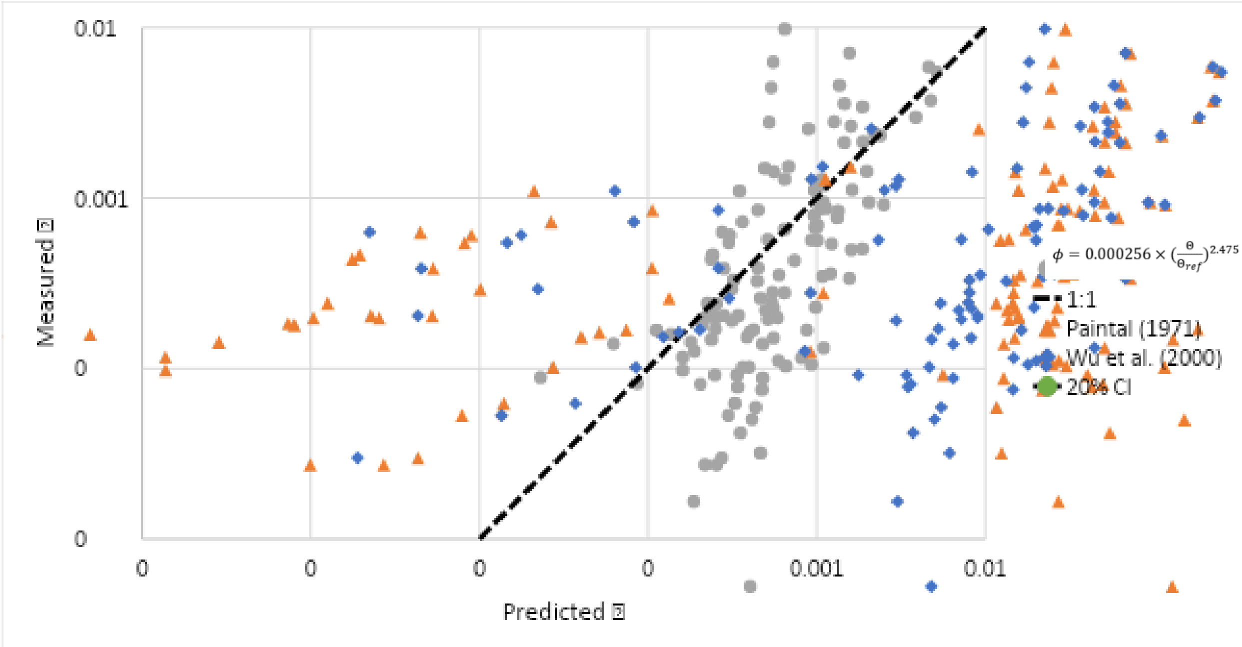

Figure 5. Comparison of the measured bedload transport rate and those calculated with the present formula and the existing formulas

Conclusions

This study investigated the effects of varying slopes and spatial densities of boulders on sediment transport. From the limited data collected in this lab, we observed an overall increase in bedload transport from increasing the slope of the channel. The boulder spacing variable saw more discrepancies across the slopes tested. The largest bedload transport was observed in the no-boulder scenarios for the 1.5% and 1% slopes, yet the no-boulder scenario recorded the lowest bedload transport during the 0.5% slope experiment. One result that is shown from the data collected from the trials was that the lowest areal density scenario (3.44%) was always the lowest recorded bedload transport out of the 3 scenarios with boulders.

Equation 7 was able to be generated to better accommodate transport rate calculations for channels with LREs present over previous open channel equations. This equation will need to be tested on other sets of data across a multitude of grain sizes before it will be reliable to calculate bedload transport rates. However, the difference shown between formulae of clear channels and equation 7, a formula designed for channels with the presence of LREs, details the limitations of some formulae that have been accepted.

Additional experiments are required to present stronger data. Multiple trials recreating these scenarios will provide replicability and additional validity to the claims made. A continuation of this research with focus on wider ranges of bed slopes and boulder areal density may also provide better insights into the study problem. Furthermore, additional parameters should be studied to further understand the ideal rock ramp structure, not limited to bed slope and boulder areal density.

References

Baki, A.B.M., Zhu, D.Z. and Rajaratnam, N. 2014. “Mean flow characteristics in a rock-ramp-type fish pass”, Journal of Hydraulic Engineering, 140(2), 156–168. https://doi.org/10.1061/(ASCE)HY.1943-7900.0000816

Golpira, A. 2022. “Effects of Instream Boulder Placement in Rock-ramp Arrangement on Local Flow with Implications for Sediment and Fish Habitats”, Clarkson University, phD Dissertation.

Ghilardi, T. and Schleiss, A.J. 2011. “Influence of immobile boulders on bedload transport in a steep flume”, in Proceedings of the 34th IAHR World Congress, edited by E. Valentine et al., pp. 3473–3480, Eng. Aust., Brisbane, Queensland, Australia.

Ghilardi, T., Franca, M. J., and Schleiss, A. J. (2014a), Bed load fluctuations in a steep channel, Water Resour. Res., Volume 50, 2014, Pages 6557– 6576, doi:10.1002/2013WR014449.

Ghilardi, T., Franca, M.J and Schleiss, A.J. 2014b. “Period and amplitude of bedload pulses in a macro-rough channel”, Geomorphology, Volume 221, 2014, Pages 95-103, ISSN 0169-555X.

Hassan, M.A. and Reid, I. 1990. “The influence of microform bed roughness elements on flow and sediment transport in gravel bed rivers.” Earth Surf. Processes Landforms 15 (8): 739–750. https://doi.org/10.1002/esp.3290150807.

Lamb M.P., Dietrich W.E., Venditti J.G. 2008. “Is the critical Shields stress for incipient sediment motion dependent on channel-bed slope?”, Journal Geophysical Research, 113, F02008, doi:10.1029/2007JF000831.

Mao, L. 2012. “The effect of hydrographs on bedload transport and bed sediment spatial arrangement”, Journal Geophysical Research, 117, F03024, doi:10.1029/2012JF002428.

McKie, C.W., Juez, C., Plumb, B.D., Annable, W.K. and Franca, M.J. 2020. “How Large Immobile Sediments in Gravel Bed Rivers Impact Sediment Transport and Bed Morphology.” *Journal of Hydraulic Engineering*, vol. 147, no. 2, 2021, https://doi.org/10.1061/(asce)hy.1943-7900.0001842.

Monsalve, A., & Yager, E.M. 2017. “Bed surface adjustments to spatially variable flow in low relative submergence regimes.” Water Resources Research, 53, 9350–9367. https://doi.org/10.1002/2017WR020845

Paintal, A.S. 1971. “Concept of Critical Shear Stress in Loose Boundary Open Channels.” Journal of Hydraulic Research, 9, 91-113. http://dx.doi.org/10.1080/00221687109500339

Papanicolaou, A.N.(T.), Tsakiris, A.G., Wyssmann, M.A. and Kramer, C.M. 2018. “Boulder array effects on bedload pulses and depositional patches.” Journal of Geophysical Research: Earth Surface, 123,2925–2953. https://doi.org/10.1029/2018JF004753

Schneider, J.M., Rickenmann, D., Turowski, J.M., Bunte, K. and Kirchner J.W. 2015. “Applicability of bedload transport models for mixed-size sediments in steep streams considering macro-roughness”, Water Resour. Res., 51, 5260–5283, doi:10.1002/2014WR016417.

Tan, L., and Curran, J. C. 2012. “Comparison of turbulent flows over clusters of varying density.” J. Hydraul. Eng. 138 (12): 1031–1044. https://doi.org/10.1061/(ASCE)HY.1943-7900.0000635.

Yager, E. M., J. W. Kirchner, and W. E. Dietrich 2007, “Calculating bedload transport in steep boulder bed channels”, Water Resour. Res., 43, W07418, doi:10.1029/2006WR005432.

Wu, W., Wang, S.S.Y, and Jia, Y. 2000. “Nonuniform Sediment Transport in Alluvial Rivers.” Journal of Hydraulic Research, vol. 38, no. 6, 2000, pp. 427–434, https://doi.org/10.1080/00221680009498296.